6A CO₂ and H₂O Gas Analyzer with Reduced Error due to Platform Motion

Douglas Vandemark, ^a Marc Emond, ^a Scott D. Miller, ^b Shawn Shellito, ^a Ivan Bogoev, ^c and Jason M. Covert ^b

^a Ocean Process Analysis Laboratory, University of New Hampshire, Durham, New Hampshire
^b University at Albany, State University of New York, Albany, New York
^c Campbell Scientific, Inc., Salt Lake City, Utah

(Manuscript received 14 November 2022, in final form 27 April 2023, accepted 28 April 2023)

ABSTRACT: One long-standing technical problem affecting the accuracy of eddy correlation air–sea CO₂ flux estimates has been motion contamination of the CO₂ mixing-ratio measurement. This sensor-related problem is well known but its source remains unresolved. This report details an attempt to identify and reduce motion-induced error and to improve the infrared gas analyzer (IRGA) design. The key finding is that a large fraction of the motion sensitivity is associated with the detection approach common to most closed- and open-path IRGA employed today for CO₂ and H₂O measurements. A new prototype sensor was developed to both investigate and remedy the issue. Results in laboratory and deep-water tank tests show marked improvement. The prototype shows a factor of 4–10 reduction in CO₂ error under typical at-sea buoy pitch and roll tilts in comparison with an off-the-shelf IRGA system. A similar noise reduction factor of 2–8 is observed in water vapor measurements. The range of platform tilt motion testing also helps to document motion-induced error characteristics of standard analyzers. Study implications are discussed including findings relevant to past field measurements and the promise for improved future flux measurements using similarly modified IRGA on moving ocean observing and air-craft platforms.

KEYWORDS: Carbon dioxide; Infrared radiation; Mass fluxes/transport; In situ atmospheric observations; Instrumentation/sensors

1. Introduction

Eddy covariance (EC) flux is one of few field measurement methods available to directly validate and refine the gas transfer models used in global estimation of CO₂ exchange between the ocean and atmosphere, and the sensor central to this measurement is typically a high-rate nondispersive infrared gas analyzer (IRGA). By necessity, air-sea EC mass flux systems are usually employed in offshore field campaigns conducted aboard research vessels where they must compensate for platform motion effects. Accurate EC CO2 flux measurement at sea requires IRGA CO2 mixing-ratio measurement precision at or below 0.2 ppm. But a well-known, persistent, and unresolved problem has been IRGA measurement error due to motion effects. Dating back to at least Fairall et al. (2000), gas transfer field experiments conducted using moving platforms have reported on the IRGA motion contamination issues as reviewed in Blomquist et al. (2014). The problem can lead to high-frequency CO₂ artifacts at 0.5-1.5 ppm levels (Miller et al. 2010).

Extensive motion-induced error correction efforts are employed in the field, including dual IRGA systems that include a separate nulling measurement system (Lauvset et al. 2011; McGillis et al. 2004) and a variety of empirical postprocessing

Openotes content that is immediately available upon publication as open access.

Corresponding author: Doug Vandemark, doug.vandemark@unh.edu

approaches (Prytherch et al. 2010; Edson et al. 2011; Miller et al. 2010; Butterworth and Miller 2016). As one estimate of observed flux error associated with this issue on a buoy platform, we calculated preliminary buoy-based estimates of EC CO₂ air-sea fluxes and averaged them across a time span with wind speeds of 5–12 m s⁻¹ and air–sea pCO₂ near +50 ppmv, yielding an average efflux near +0.5 mmol m⁻² h⁻¹. If the IRGA CO2 (Campbell Scientific EC155 in this case) data were left uncorrected, then the estimated mass flux had the wrong sign and a magnitude triple of that expected. If motion-compensated using the approach of Miller et al. (2010), then we obtained a 35% negative bias. This flux error is of similar order, but exceeds the 10%-15% error inferred from motion-corrected shipboard results shown in Fig. 6 of Edson et al. (2011). And while reasonable motion-corrected EC results are often obtainable at sea, especially in higher gas transfer rate environments, progress on the core technical IRGA measurement error issue has not been made.

Numerous investigators have speculated on the root cause of IRGA motion sensitivity. These include mechanical deformation of the optical path (Yelland et al. 2009), source filament flex (Miller et al. 2010), and chopper wheel instabilities (McGillis et al. 2001a), with common themes being variable performance depending on sensor orientation, open-path versus closed-path IRGA, and specific platforms and deployments. All field measurements reported to date on the motion-induced error issue have used some version of IRGA from LI-COR Biosciences Inc. (models LI-7000, LI-7200, LI-7500, and LI-6262). A further complication to identifying specific IRGA error sources are the potentially intertwined issues of the sensor-specific measurement cell pressure variations and CO₂ crosstalk

DOI: 10.1175/JTECH-D-22-0131.1

corrections tied to the water vapor measurement (Blomquist et al. 2014).

Our group had an interest in deploying a closed-path IRGA on research buoys for EC CO₂ mass flux measurements with the expectation that past motion corrections methods could be successfully employed. An EC system with a dried sample line and closed-path LI-7200 sensor, similar to that used in shipboard studies, was developed and deployed on an offshore air–sea flux buoy in 2014. A main lesson taken from those field trial data was that discus buoy motions, often much larger and more erratic than encountered on large research vessels, led to greater IRGA CO₂ mixing-ratio errors than previously reported, and errors that were uncorrectable using proposed empirical postprocessing methods (Miller et al. 2010; Edson et al. 2011; Prytherch et al. 2010).

Further investigation of the sensor itself after deployment, as well as an available open-path LI-7500 unit, led to the observation that much of the CO2 motion contamination signal was correlated with a detector temperature control voltage associated with the receive end of the sensor. As an example, Fig. 1 provides frequency cospectra of CO2 mixing-ratio and receiver (Rx) control voltage measurements derived from fixed and moving 20-Hz measurement time series collected in similar winds and air-sea CO₂ environments. In one case the buoy is on a pier with no motion, and in the other it is moored 6 mi (\sim 10 km) offshore from the pier under wind-wave forcing. The sample line into the LI-7200 sensor was dried to limit water vapor contamination. The average buoy pitch and roll tilting angles were 8.5° for these 7 m s⁻¹ wind speed conditions, and the tilt spectra in Fig. 1 show the nominal buoy motion frequency band lies between 0.2 and 0.7 Hz. The CO2-Rx voltage covariance under motion within this band is apparent and at least 7 times as large as outside the motion pass band, whereas the fixed-platform measurements under similar winds show no obvious correlation with detector control signals. Attempts to develop an empirical solution to correct the field deployment CO₂ measurements using the detector control voltage time series data were not successful, but these observations did lead us to focus on the IRGA receiver as a potential root cause of the motion contamination problem and they also motivate the work to be presented.

This study summarizes the development of a modified NDIR gas analyzer designed to reduce motion-induced CO₂ errors and documents improved performance under a range of controlled platform motion tests. Methods are described in section 2 including initial motion-table measurements used to optimize analyzer modifications, a subsequent full-scale buoy-mounted experimental tank test setup, and approaches chosen for end-to-end water vapor and CO₂ data assessment. Section 3 summarizes results and section 4 discusses implications for past and future eddy covariance mass flux measurements on moving platforms.

2. Methods

a. Trace gas analyzers and supporting measurements

This paper focuses on assessments of and improvements to a standard commercially available IRGA, the EC155 from Campbell Scientific, Inc. (CSI). The EC155 is a closed-path

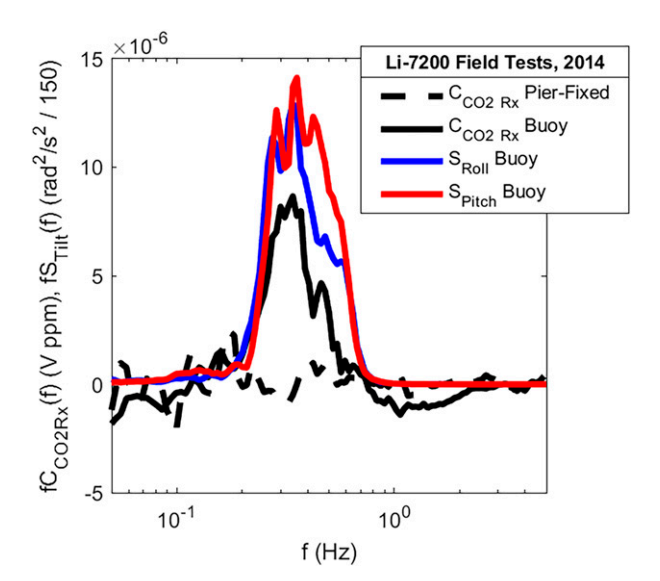


FIG. 1. Cospectra of CO₂ mixing ratio and IRGA detector cooler voltage obtained from separate tests, showing moving- vs fixed-platform results. The two October 2014 buoy datasets were collected in the coastal Gulf of Maine using an off-the-shelf closed-path IRGA (LI-7200). Wind speed was 7 m s⁻¹ for both cases, and cospectra are derived using 10-min data segments. Also shown are the autospectra of buoy pitch and roll motions for the moving case. The fixed-platform data were collected with the buoy standing on a pier at the University of New Hampshire Coastal Marine Laboratory.

system used in a wide range of environmental field measurement applications (Novick et al. 2013; Ma et al. 2017). The sensor's primary purpose is to provide high-rate and high-precision CO₂ and H₂O mixing-ratio measurements, where the desired data sampling rates are 5-20 Hz and their specified CO2 and H₂O measurement precision is 0.15 µmol mol⁻¹ and 0.006 mmol mol⁻¹, respectively. The EC155 also provides high precision temperature and pressure measurements inside the closed-path sample cell to adjust for ambient impacts on the flow when converting from the raw molar density measurements to mixing ratio. While the EC155 field sample air collector employs a vortex intake device, this intake is bypassed in this study because of the sole focus on motion-induced noise associated with the analyzer itself. EC155 control, transducer sampling, and data conversions are performed using a CSI EC100 electronics unit, and a CSI CR6 data acquisition system was used to collect the measurements for all experiments.

The basic theory of operation for the EC155 nondispersive IR gas analyzer is outlined in the CSI product manual. It follows the approach of Heikinheimo et al. (1989) where a broadband infrared source is transmitted through a gas sample volume via a rotating chopper wheel controller that modulates the source signal at a high rate, alternating between signal and dark (null or reference) source levels. An IR detector at the receiving end of the volume is aligned to measure IR radiation changes for the repeating source and dark reference levels, with the detected IR levels changing with gas absorptance due to volumetric change in carbon dioxide and water vapor inside

the sample cell. The lowest (raw) level detector measurements within several separate IR bands provide the demodulated light and dark reference data used to calculate the mixing ratios for both gases.

The hardware developed for this project is an altered version of the EC155 analyzer. As noted above, the hypothesis is that IRGA motion-induced error is primarily associated with issues related to the infrared detection section of the analyzer rather the transmitter (source) end of the sensor. A miniaturized millimeter-scale IR photodetector within any similar IRGA is central to both CO₂ and H₂O gas absorption measurements, and it must be operated at a cold temperature near -40°C. This is done using an integrated three- or four-stage thermoelectric cooler. Detector temperature control responds to changes measured at a small thermistor mounted next to the detecting element. Our working hypothesis is that platform-induced detector measurement error is largely due to small, rapid, and often unpredictable thermally induced convective temperature change within the hermetically sealed solid state photodetector device. Monitoring thermoelectrically cooled (TEC) control voltage during simple physical motion manipulation of the analyzer's detector while the rest of the IRGA is fixed suggests that this is the case. The orientation of the thermistor and the detection element relative to each other and to gravity apparently factor into how specific platform rotations (e.g., pitch vs roll) and accelerations induce IRGA error. These detectors are typically purged and filled with gas, and this is the conductive medium that varies with buoyancy forcing caused by motion.

The key new IRGA modification is to employ a similar photodetector unit, but one that has been fully evacuated. The expectation is that this will eliminate the convection and, in turn, the coupled detector/thermal control variations that lead to gas measurement error. This detector modification was implemented in a breadboard EC155 unit without other substantial changes to the established EC155 mechanical and optoelectrical design, data handling and output, and sensor control. This prototype unit is denoted as EC155P in this paper. The limited scope of modifications means that side-by-side evaluation of this new EC155P versus the standard EC155 unit is straightforward, simplifying the quantification of sensor performance differences.

While this study does not report on similar motion tests that were carried out using off-the-shelf LI-COR Biosciences LI-7200 and LI-7500 closed- and open-path IRGA analyzers, we have observed that the magnitude and characteristics of motion-induced errors using these sensors is on the order of the EC155 results to be presented, and are consistent with that observed in past studies (cf. Lauvset et al. 2011, and references therein). This is not surprising given that much of the IRGA measurement approach, design, and electromechanical implementation is similar between the two instrument manufacturers.

One of two inertial motion measurement packages was employed to log platform motion data in these tests (Parker Lord Microstrain 3DM-GX3 or 3DM-GX5). Either provides dynamic attitude data at a 20-Hz sampling rate coincident with our IRGA measurements. The motion sensor was aligned and mounted on the rigid IRGA test plate adjacent to the

analyzers. All platform pitch, roll, and acceleration estimates were derived using standard postprocessing approaches employed at sea (Edson et al. 1998; Miller et al. 2010).

All recorded datasets include continuous high-rate measurements of all standard EC155 output variables including cell temperature and pressure, additional low-level EC155 engineering outputs, and motion sensor outputs including three-axis accelerations and angular rotation rates. Most data presented were recorded at a 20-Hz sampling rate. EC155 and EC155P CO₂ and H₂O outputs were low-pass filtered prior to datalogging using the recommended EC155 bandwidth of 10 Hz. The sensor error evaluation always involved a simple approach of measuring a continuous stream of nearly pure (dry) CO₂ reference gas flowing through the system, typically at a controlled 0.7-1.5 lpm flow rate. Evaluation of prototype differences with the standard EC155 sensor is primarily made via direct comparison of time series measurements or derived noise variance of the CO₂ and H₂O mixing-ratio data observed in frequency ranges associated with the platform motion from the simultaneously recorded motion sensors.

b. Bench and dive tank motion impact assessments

Simple two-axis and dynamic three-axis motion-table tests were employed to diagnose, improve, and evaluate EC155 measurement noise associated with platform tilting motion having magnitudes and frequencies expected at sea. In all tests, sensor CO2 and H2O mixing-ratio errors were assessed by sampling intake gas having a known fixed CO₂ concentration drawn through the IRGA measurement sample cell at a flow rate typical for field measurements (Lauvset et al. 2011). The CO₂ reference gas was dry (effectively no water vapor) and the level was either 500 or 520 ppm. The two-axis motion tests were first performed to individually evaluate rotation (pitch or roll) effects. The laboratory motion table consisted of a stiff 1.2 m × 1.2 m plate with one free axis of rotation about the center, and where both the EC155 and EC155P were mounted side by side, centered atop that rotational axis and in the same horizontally mounted orientation along with the motion sensor. Note that CSI recommends horizontal mounting of the EC155, in part to maintain consistency with their factory calibration approach. To assess motion impacts for the orthogonal tilt (i.e., roll instead of pitch), the table was physically rotated on the stand by 90°. The sensor input sample gas was plumbed in series, running through the EC155P and then the EC155. All measurements were recorded simultaneously using the CSI CR6 datalogger.

A series of rotation tests were conducted at varying pitch and roll levels to assemble IRGA measurement datasets that span a range of expected field tilt amplitudes (from 0° to 20° in pitch and roll typical of discus buoy platforms), and using an average rotation rate of 0.33 Hz that lies near the fundamental resonance frequency of our specific air–sea flux buoy. The footprint of each EC155 is rectangular (7 cm \times 43 cm), and in our testing framework a roll-impacted measurement implies rotation about the long axis and pitch about the short. This two-axis (2D) test was fashioned after a motion impact

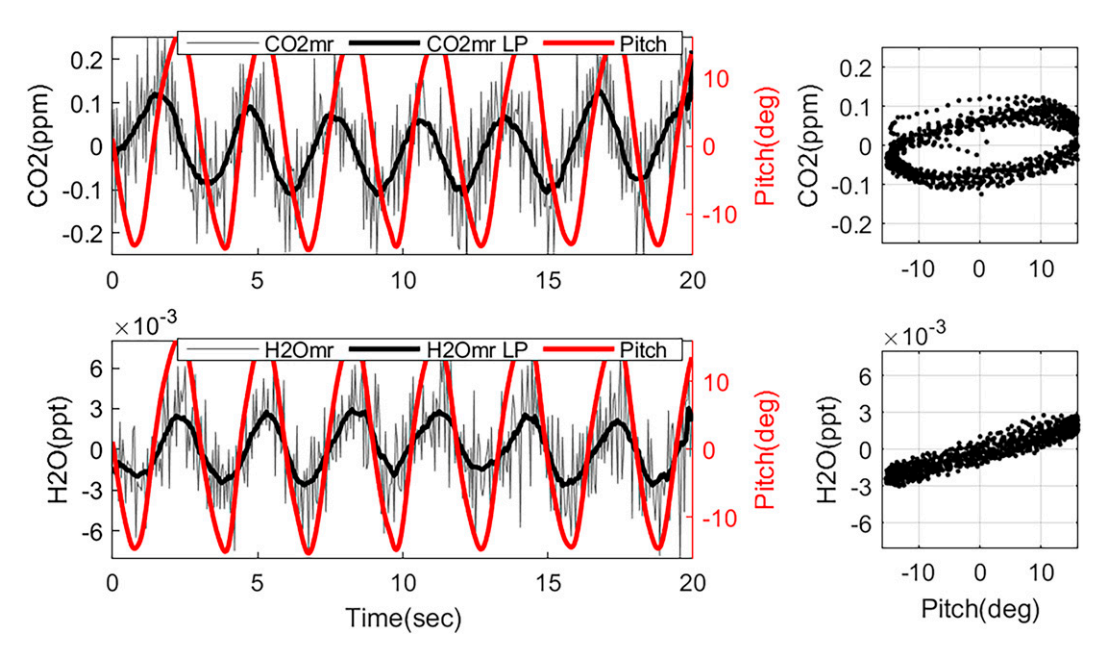


FIG. 2. (left) Laboratory motion-table test data showing standard EC155 (top) CO_2 and (bottom) H_2O molar mixing-ratio variation with time while platform pitch (in red) is modulated. CO_2 and H_2O mean levels have been subtracted. Both the raw 20-Hz (thin black) and low-pass-filtered (thick black) data are shown. The platform rotation rate was roughly 0.35 Hz. (Right) Corresponding scatterplots of the low-passed mixing-ratio data vs the instantaneous tilt angle. Pitch variations are $\pm 15^{\circ}$.

assessment of LI-COR IRGA units performed at NOAA's Earth System Research Laboratories in 2010 by L. Bariteau.

Figure 2 illustrates pitch-induced error observed in both CO₂ and H₂O when using the standard EC155 in these 2D table tests. A short test segment with a few platform oscillations is shown including the measured platform tilt and mixing-ratio data at the raw 20-Hz rate and after low-pass filtering. The mean CO2 and H2O levels are subtracted to focus on the relevant small-scale signal variations. Results clearly show high correlation between platform tilt and mixing-ratio measurements. This test was for repeated pitch motions of ±14°. Higher-frequency (>1 Hz) CO₂ sensor noise is evident, and the measured root-mean-square (rms) noise level is 0.047 ppm. The Fig. 2 pitch-induced signal amplitude estimated using the smoothed curve is near 0.12 ppm peak to peak, a factor of at least 2 above the noise. The EC155 motion-induced signal is clear. The variations are also consistent with, but in this case smaller than, the 0.5-2.0 ppm signals noted in previous field studies (cf. Fig. 5 in Miller et al. 2010). A similar tilt-related increase above the noise level is observed for H₂O. The high correlation between the motion and IRGA error suggests linearity, but the right panels show an apparent systematic hysteresis, more evident in the CO₂ than the water vapor in this case.

Figure 3 shows similar data but for roll rotations (tilting the EC155 side to side). In this case, the roll-induced CO_2 signal amplitude is similar, but the hysteresis differs with CO_2 error versus pitch results. As seen in Fig. 3b, the CO_2 variation with the roll is more linear. In both pitch and roll cases it is evident that EC155 water vapor and CO_2 motion-induced errors do

not track with the induced motions in the same manner. Such a result is inconsistent with the suggestion that motion-related errors for H_2O and CO_2 are highly correlated for the same sensor (Edson et al. 2011).

Similar hystereses between the mixing-ratio and tilt-angle time series data were observed in all study tests, and they become increasingly nonlinear once 3D motions and more varied platform motion frequencies are allowed. This implies that simple tilt-related data correction approaches would be problematic even on less dynamic platforms, for example, those subject to mostly pitching motions like a glider or ship or for an aircraft to roll. Further data and discussion on pitch-and roll-induced noise for the EC155 and EC155P will be provided in following sections.

The single-axis rotation bench test configuration was also used to examine and document both EC155 and EC155P CO₂ measurement performance change under motion due to other potential and suggested IRGA system factors. This included investigation of the water vapor cross talk correction, varied source filament power level, cell pressure corrections, varied chopper wheel rotation rate, varied measurement sampling rate, optical bench rigidity, mean detector temperature, and physical orientation of the sensor. Access to, and assessment of, additional low-level EC155 engineering variables aided in this process. Most of these factors did not markedly alter EC155 sensitivity to motion. Exceptions were the sensor mounting orientation and optical bench rigidity. Several of these factors will be revisited in the discussion section.

A similar fixed-plate configuration was used for three-axis motion tests intended to simulate field measurement conditions

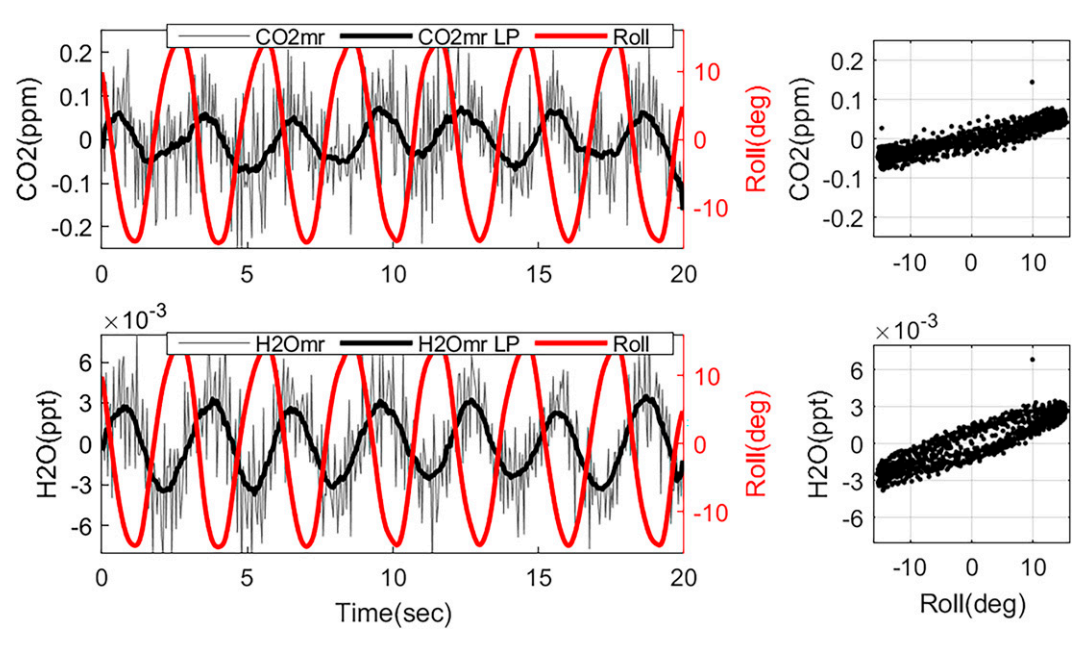


FIG. 3. As in Fig. 2, but for $\pm 15^{\circ}$ in roll.

more closely. The two-sensor test plate was mounted directly onto the center of a 2 m discus buoy platform as shown in Fig. 4. A $\rm CO_2$ reference gas tank was strapped to the buoy and the entire platform was then floated in an 8-m-deep ocean instrument test tank located in the Chase Engineering Laboratory at the University of New Hampshire. Both periodic and irregular platform motions were induced by coordinated manipulation of the buoy (see Fig. 4) from multiple sides with the buoy centered in the large tank. The approach allowed simulated time series data collection with platform pitch and roll tilting rates near the nominal buoy resonant frequency (f = 0.33 Hz) and with variation in the mean level of tilt. Tests with mean pitch and roll

variations in the range from 3° to 15° were performed reflective of low to high wind conditions measured in recent buoy deployments, where a rms tilt angle, $\sigma_{\rm tilt}$, of 8° is nominal for wind speeds of 9 m s⁻¹. Mixed (or confused) sea conditions more typical of actual adverse field situations were also achieved with this setup by more random forcing of the platform. Typically, 2–3 min of continuous data were collected for a given motion test (e.g., $\sigma_{\rm tilt} = 5^{\circ}$ in roll). This permits characterization of motion-induced noise at different mean tilt angles. One known forcing that was not simulated with this setup was strong vertical platform accelerations (heave) associated with typical sea states that may also induce noise (Miller et al. 2010).



FIG. 4. (left) Test configuration for the discus buoy motion for the deep-water dive tank tests. (right) A view looking down at the buoy tower center plate where the EC155 (stock model) and EC155P (prototype) IRGA sensors are mounted to the same horizontal test panel. The plate is 1.3 m above the water line and over the center of rotation.

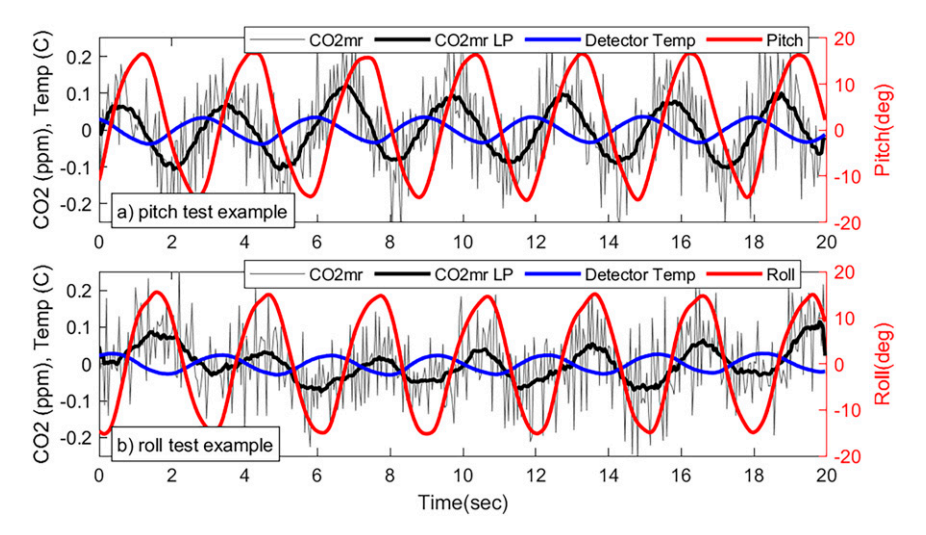


FIG. 5. Standard model EC155 time series data similar to Figs. 2 and 3, but only showing CO_2 IRGA data and with the addition of time variation in EC155 detector temperature after subtracting its mean level. Average pitch and roll variations are $\pm 10^{\circ}$ to 12° : (a) pitch-only motion and (b) roll-only motion.

3. Results

a. Primary source of motion-induced IRGA error

Similar to Miller et al. (2010), laboratory experimentation with various IRGA units including the EC155 were undertaken to examine sensor-related causes for motion-induced measurement changes such as that seen in Figs. 2 and 3. Experimental approaches to assess motion sensitivity to the sensor mounting orientation, chopper wheel rotation speed, remaining high-frequency pressure related noise, water vapor cross talk correction, radiation source variability, optical bench flexure, and receiver performance were devised and conducted using access to engineering level measurement data collected during both bench and tilt table testing.

These tests indicate that the dominant source of tilt-related error is associated with analyzer IR signal detection. This was already indirectly illustrated in Fig. 1 using LI-7200 detector cooler voltage data. The EC155 provides high-rate measurements of the temperature associated with the TEC IR sensor detector. Figure 5 shows standard model EC155 data from short 20 s measurement segments during separate buoy pitch and roll motion tests ($f \approx 0.35$ Hz) in the deep-water tank. Both tests show EC155 detector temperature data (in blue) have frequency variations with amplitude of 0.1° – 0.2° C that are visibly elevated in the roll tests. The variations are anticorrelated with tilt, but slightly out of phase with the motion. There is also an apparent detector temperature correlation, but also a phase shift with respect to the CO₂ measurement change, most evident in the smoothed CO₂ signal.

This motion-correlated change in CO₂ and H₂O data is observed versus detector temperature in all platform tilt and acceleration tests, but with varying amplitude and phase shifts. Empirically, it is clear that there is fairly high nonlinearity between the control temperature, the motion, and the trace gas measurements. This is likely related to the observed hysteresis

between mixing ratio and platform tilt variation shown in Figs. 2 and 3.

The EC155P is modified to address this issue. Results from side-by-side tests of EC155P versus EC155 performance are shown in Fig. 6. Pitch test data are shown in the upper panel and the bottom is roll. The dramatic decrease in EC155P TEC temperature variation versus the EC155 is clear. In fact, the EC155P appears to be 0.0 as there is effectively no measurable high-rate TEC variation in the prototype, whereas the EC155 again shows 0.1°C variations. What is most encouraging is the evident improvement in motion-related EC155P CO₂ mixing-ratio signal. While not completely removed, the CO₂ signal variation at the tilting frequencies is reduced by at least a factor of 4-5. There is also a clear phase shift in the motion impacts on CO₂ between the EC155 and EC155P indicating a fundamental change between the two sensors. One additional observation is that larger EC155 TEC and CO2 variations are observed under pitch motions than for roll consistent with Fig. 5. Similar impacts are observed in the H₂O channel data (not shown). This complete attenuation of TEC temperature variation correlated with sensor motion was observed across the full range of tilt motion tests conducted.

The EC155P results confirm our expectation that improved detector stabilization leads to reduced motion contamination in IRGA CO_2 and H_2O measurements.

b. EC155P performance in variable motion tests

To further document and summarize EC155P performance change with respect to the stock EC155 unit, a motion-induced error (MIE) metric is formulated to accurately quantify the level of motion-induced CO₂ or H₂O error. MIE is defined using the ratio of signal variation when under motion to measurements collected with no motion, i.e., the static case. The calculation is performed in the spectral domain across the motion frequency pass band encountered in the buoy wave tank

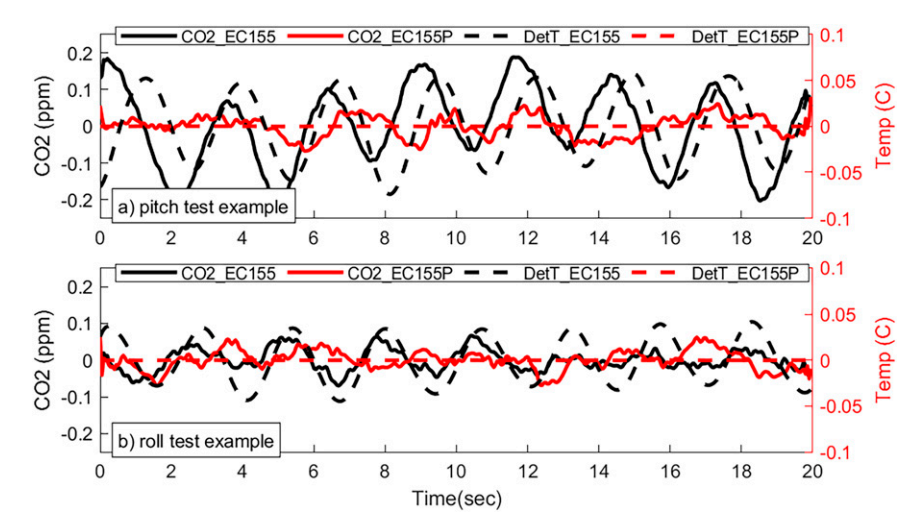


FIG. 6. Standard and prototype (EC155 and EC155P) time series data showing bandpass filtered variation in CO_2 and detector temperature data after subtracting mean levels: (a) Pitch test data, and (b) roll. Variations are $\pm 10^{\circ}$ –12°.

tests (from $f_{\text{Lo}} = 0.2$ to $f_{\text{Hi}} = 0.6$ Hz). This accounts for the inherent noise of each individual sensor when the platform is fixed. An MIE level approaching one means no motion impact on a given measurement:

$$MIE = \frac{\int_{f_{Lo}}^{f_{Hi}} S(f) df}{\int_{f_{Lo}}^{f_{Hi}} S_{\text{static}}(f) df}.$$
 (1)

Here S(f) is either the CO_2 or H_2O spectral density for a given motion test segment. MIE is calculated for each of many 60–120 s measurement test segments, where the platform tilt standard deviation for each segment is computed as $\sigma_{\text{Tilt}} = \sqrt{\sigma_{\text{pitch}}^2 + \sigma_{\text{roll}}^2}$. Example spectra for one mixed sea motion test set are shown in Fig. 7. The large EC155 CO_2 signal increase in the pass band versus the static case is evident, while the prototype level is much closer to its noise floor. Note that static-case EC155P noise level slightly exceeds that of the EC155, even in the pass band. As one measure of the difference, the rms CO_2 noise level above 1 Hz for the EC155 is 0.047 while the EC155P is 0.068 ppm. This is a known prototype limitation that is unrelated to motion improvement goals and could be improved in the future.

Summary of side-by-side sensor measurements under varied motion is provided in Fig. 8 including separate pitch, roll, and mixed sea segments. Buoy tilting motions are always present and thus the platform never provides $\sigma_{\rm tilt}$ levels below 3°–4°. The largest sensor error is seen for pitch motion in the EC155, with MIE increasing from 4 to 11 for tilt amplitudes of 5°–15°. This is 3–4 greater error than is seen for EC155 roll motion error. EC155 error shows a quasi-linear increase with increasing tilt amplitude for pitch, roll, or mixed motions. The difference between the EC155 and the new prototype is apparent in all cases. The EC155P has much lower MIE that never exceeds 1.1 and there is no evident MIE increase with increasing $\sigma_{\rm tilt}$.

The mixed sea test data at right in Fig. 8 represent the net effect of anticipated buoy tilt impacts on CO_2 error in the field. One measure of prototype improvement is the ratio of the EC155 to EC155P signal for a given motion test segment, i.e., MIE_{EC155}/MIE_{EC155P} . Using this, the observed EC155P improvement versus the EC155 is 3.6–6.2 times for σ_{tilt} below 8° and as much as 10.4 for the highest tilt. The average improvement factor is 5.2.

Water vapor channel data are shown in Fig. 9. They demonstrate overall EC155P improvement by a factor of 2–8, but the results differ somewhat from the CO₂ data. First, at left,

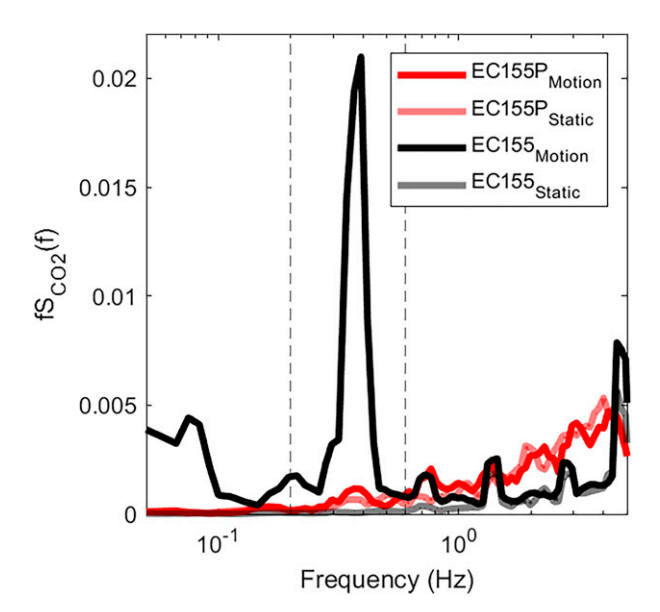


FIG. 7. Autospectra of CO_2 measurements during both static platform and mixed sea motion tests. The platform σ_{tilt} for this segment was 10° . Frequency bandpass limits for MIE calculations are shown with vertical dashed lines.

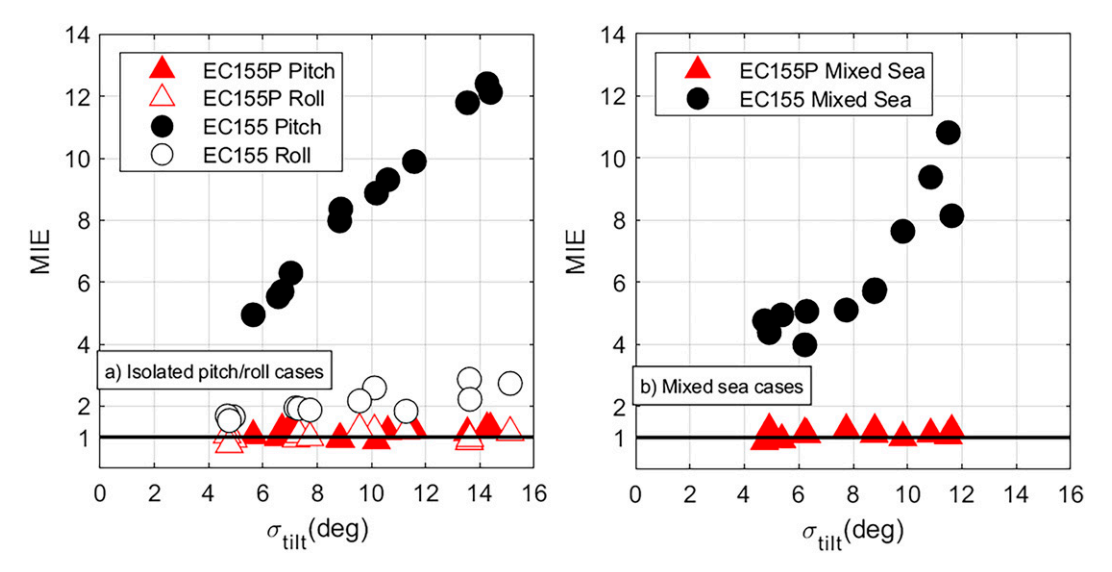


FIG. 8. Summary of CO_2 motion-induced error during tank measurements. Each test segment had a differing mean tilt amplitude σ_{tilt} . (left) Pitch or roll motion test results for both the EC155 and EC155P. (right) The mixed sea motion results under increasing tilt. MIE, the effective motion-related error factor above the noise floor, is defined in Eq. (1).

the EC155 pitch-induced H_2O response is similar to the CO_2 data in Fig. 8. But the roll-induced wsignal is significantly elevated relative to CO_2 . Second, prototype H_2O measurement error is also evident and it also increases with $\sigma_{\rm tilt}$, though at a much lower overall level than the EC155. Pitch test EC155P MIE ranges from just above 1.3 at $\sigma_{\rm tilt}$ of 5.5° to 3.2 at $\sigma_{\rm tilt}$ above 14°. EC155P roll error is smaller than pitch error by a factor of roughly 3. The overall prototype H_2O improvement versus the EC155 is again quantified using the mixed sea test results at right in Fig. 9. They indicate that the average EC155P improvement level is 3.5, ranging from 1.6 to 8.5 across the varied motion amplitude tests.

4. Discussion and conclusions

The primary study finding is that receiver-end modifications to a standard chopper wheel type IR trace gas analyzer reduces the motion-induced error due to platform tilt by a factor of 3.6–10.4 in the CO_2 channel and by 1.6–8.5 in the water vapor channel. This new EC155P unit also showed no measurable increase in CO_2 error as platform tilt amplitudes were increased, or when varying the orientation of the applied rotations. This significant level of improvement suggests that the closed-path IRGA approach to trace gas measurements may yet be able to attain CO_2 field measurement precision approaching that of the cavity ring down spectrometer (Blomquist et al. 2014) and permit accurate

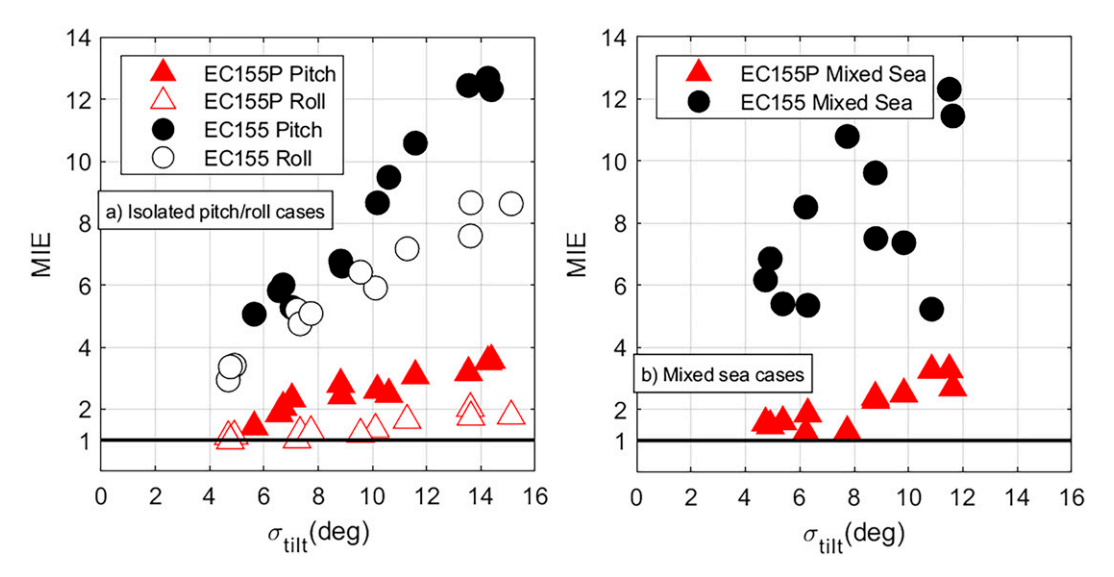


FIG. 9. Summary of the H₂O motion-induced error metric for the same test series as Fig. 8.

 ${\rm CO_2}$ mass flux measurements when the air–sea pCO₂ disequilibrium is well below the presently assumed IRGA EC flux baseline level of 40–50 μ Atm (Rowe et al. 2011). Moreover, this hardware improvement should aid efforts to more clearly isolate, diagnose, and improve other fundamental and critical high-rate IRGA ${\rm CO_2}$ corrections such for the cell pressure and ${\rm CO_2}$ and ${\rm H_2O}$ channel cross talk.

Study results also indicate that platform motion impacts on standard-model IRGA analyzer (EC155) measurement error have several clear characteristics. Error increases with platform tilt amplitude, it varies with the tilt direction relative to sensor mounting orientation, it varies nonlinearly with platform tilt, and it shows a correlation with sensor detector temperature control data. While most of the presented data focused on CO₂ measurements, these four characteristics were similarly observed in the H₂O data. Each of the first three characteristics have been mentioned or alluded to in previous literature discussing platform motion effects. In particular, our finding of significantly enhanced error amplitude under pitch as compared with roll rotations is consistent with the understanding that one should optimize the sensor mounting orientation to limit error on any particular platform or field deployment (cf. Yelland et al. 2009). This new EC155P sensor removes or significantly reduces nearly all of these error-related characteristics.

One study implication is that much of the error seen in previous experiments is related to IRGA receiver error. And it is hypothesized that at least some of the strengths and weaknesses of past empirical IRGA CO2 motion correction approaches using platform motion data are related to the physical orientation of the sensor receiver with respect to the applied motions. For example, if ship pitching motions dominate the sensor forcing and the sensor is mounted such that pitch-induced error is enhanced, then correction becomes more problematic. Similarly, reconsideration of motion impacts observed in these previous CO₂ flux studies might benefit from a review of sensor mounting orientation with respect to a given platform's dynamics as well as to high-rate data associated with the IR detector inside a given sensor. This study focused primarily on the CSI EC155, but as shown in Fig. 1, the LI-COR IRGA units often output high-rate detector cooler voltage information that could be useful to diagnose improve the quality control of cases with large or unexplained error due to platform motion. Results of Figs. 2, 3, and 8 document some of the observed nonlinear relationships between varied platform tilting and observed trace gas measurement error. We found no reliable approach for platform motion correction as varied rotational motions and resulting nonlinearities increase.

A further implication is that the approach to use a second closed-stream nulling IRGA unit to correct the primary science sensor (Lauvset et al. 2011; McGillis et al. 2001b; Edson et al. 2011) is suboptimal unless one considers this mounting orientation issue for both units, but more so because our anecdotal findings, informed by discussions with manufacturers, were that each individual sensor has a unique error response to motions even when of the same IRGA model. This is consistent with (Yelland et al. 2009). We anticipate that the new

receiver modification approach would lessen the variability in same-model sensor response to motion.

Similar infrared detectors are not only used in nondispersive infrared gas analyzers, but also in other state-of-the-art trace gas laser-based gas analyzers including the CSI TGA200A, cavity ring-down spectrometers (CRDS), and off-axis integrated cavity output spectrometers (OA-ICOS). Consequently, such analyzers may also be prone to platform motion-induced $\rm CO_2$ and water vapor measurement error. In broader terms, methane and n+itrous oxide analyzer measurement performance might also be improved via implementation of thermally stabilized IR detectors.

The EC155P performance already shows promise for improved use of IRGA for air–sea flux measurements, but the unit was only built as a bench top prototype to assess the benefit of receiver modifications. Prototype design decisions explain part of the small remaining motion-related noise observed, for example, in the water vapor measurements of Fig. 9, and slightly elevated high-frequency noise in Fig. 5. Thus, several known and relatively minor additional design changes should further enhance the performance of a fully field ready unit. Diagnosis of some of these design decisions benefited from error reduction provided by the EC155P detector changes.

A forthcoming companion study will report on 2021 offshore ocean field trials conducted using the same buoy and the same side-by-side EC155 versus EC155P measurement design, along with its integration into a full EC flux system. Those field data will allow EC155P performance assessment under significant platform heave conditions, tests that were not performed in this investigation. That study that will also assess IRGA trace gas and eddy correlation flux measurement improvements under varied wind, wave, atmospheric CO₂, and air–sea CO₂ flux conditions.

Acknowledgments. We thank Rex Burgon and Joseph Kimchi for their assistance with EC155P sensor development. This work was supported by NSF Ocean Technology and Interdisciplinary Coordination program Awards 1737328 and 1737184.

Data availability statement. Study datasets and source code used to create all figures are provided in a compressed file folder that is available online (https://www.opal.sr.unh.edu/data/IRGA_with_motion_sensitivity.zip).

REFERENCES

Blomquist, B. W., B. J. Huebert, C. W. Fairall, L. Bariteau, J. B. Edson, J. E. Hare, and W. R. McGillis, 2014: Advances in air–sea CO₂ flux measurement by eddy correlation. *Bound.-Layer Meteor.*, 152, 245–276, https://doi.org/10.1007/s10546-014-9926-2.

Butterworth, B. J., and S. D. Miller, 2016: Automated underway eddy covariance system for air–sea momentum, heat, and CO₂ fluxes in the Southern Ocean. *J. Atmos. Oceanic Technol.*, **33**, 635–652, https://doi.org/10.1175/JTECH-D-15-0156.1.

- Edson, J. B., A. A. Hinton, K. E. Prada, J. E. Hare, and C. W. Fairall, 1998: Direct covariance flux estimates from mobile platforms at sea. *J. Atmos. Oceanic Technol.*, **15**, 547–562, https://doi.org/10.1175/1520-0426(1998)015<0547:DCFEFM> 2.0.CO;2.
- —, and Coauthors, 2011: Direct covariance measurement of CO₂ gas transfer velocity during the 2008 Southern Ocean Gas Exchange Experiment: Wind speed dependency. *J. Geophys. Res.*, 116, C00F10, https://doi.org/10.1029/2011JC007022.
- Fairall, C. W., J. E. Hare, J. B. Edson, and W. McGillis, 2000: Parameterization and micrometeorological measurement of airsea gas transfer. *Bound.-Layer Meteor.*, 96, 63–106, https://doi.org/10.1023/A:1002662826020.
- Heikinheimo, M. J., G. W. Thurtell, and G. E. Kidd, 1989: An open path, fast response IR spectrometer for simultaneous detection of CO₂ and water vapor fluctuations. *J. Atmos. Oceanic Technol.*, 6, 624–636, https://doi.org/10.1175/1520-0426(1989)006<0624:AOPFRI>2.0.CO;2.
- Lauvset, S. K., W. R. McGillis, L. Bariteau, C. W. Fairall, T. Johannessen, A. Olsen, and C. J. Zappa, 2011: Direct measurements of CO₂ flux in the Greenland Sea. *Geophys. Res. Lett.*, 38, L12603, https://doi.org/10.1029/2011GL047722.
- Ma, J., and Coauthors, 2017: An eddy-covariance system with an innovative vortex intake for measuring carbon dioxide and water fluxes of ecosystems. *Atmos. Meas. Tech.*, 10, 1259– 1267, https://doi.org/10.5194/amt-10-1259-2017.
- McGillis, W. R., J. B. Edson, J. E. Hare, and C. W. Fairall, 2001a: Direct covariance air-sea CO₂ fluxes. *J. Geophys. Res.*, **106**, 16729–16745, https://doi.org/10.1029/2000JC000506.

- —, —, J. D. Ware, J. W. H. Dacey, J. E. Hare, C. W. Fairall, and R. Wanninkhof, 2001b: Carbon dioxide flux techniques performed during GasEx-98. *Mar. Chem.*, 75, 267–280, https://doi.org/10.1016/S0304-4203(01)00042-1.
- —, and Coauthors, 2004: Air-sea CO₂ exchange in the equatorial Pacific. J. Geophys. Res., 109, C08S02, https://doi.org/10.1029/2003JC002256.
- Miller, S. D., C. Marandino, and E. S. Saltzman, 2010: Ship-based measurement of air-sea CO₂ exchange by eddy covariance. *J. Geophys. Res.*, 115, D02304, https://doi.org/10.1029/2009JD012193.
- Novick, K. A., J. Walker, W. S. Chan, A. Schmidt, C. Sobek, and J. M. Vose, 2013: Eddy covariance measurements with a new fast-response, enclosed-path analyzer: Spectral characteristics and cross-system comparisons. *Agric. For. Meteor.*, **181**, 17– 32, https://doi.org/10.1016/j.agrformet.2013.06.020.
- Prytherch, J., M. J. Yelland, R. W. Pascal, B. I. Moat, I. Skjelvan, and M. A. Srokosz, 2010: Open ocean gas transfer velocity derived from long-term direct measurements of the CO₂ flux. *Geophys. Res. Lett.*, 37, L23607, https://doi.org/10.1029/2010GL045597.
- Rowe, M. D., C. W. Fairall, and J. A. Perlinger, 2011: Chemical sensor resolution requirements for near-surface measurements of turbulent fluxes. *Atmos. Chem. Phys.*, 11, 5263–5275, https://doi.org/10.5194/acp-11-5263-2011.
- Yelland, M. J., R. W. Pascal, P. K. Taylor, and B. I. Moat, 2009: AutoFlux: An autonomous system for the direct measurement of the air-sea fluxes of CO₂, heat and momentum. *J. Oper. Oceanogr.*, 2, 15–23, https://doi.org/10.1080/1755876X. 2009.11020105.